Extreme Mechanics Letters 46 (2021) 101348

Contents lists available at ScienceDirect

Extreme Mechanics Letters

journal homepage: www.elsevier.com/locate/eml

Ventilated metamaterials for broadband sound insulation and tunable transmission at low frequency

Zhenqian Xiao [a,1], Penglin Gao [b,1], Dongwei Wang [c], Xiao He [d,*], Linzhi Wu [a,d,**]

[a] Center for Composite Materials, Harbin Institute of Technology, 150001 Harbin, China
[b] Department of Physics, Universidad Carlos III de Madrid, ES 28916, Leganès, Madrid, Spain
[c] School of Aerospace Engineering, Beijing Institute of Technology, 100081 Beijing, China
[d] Key Laboratory of Advanced Ship Materials and Mechanics, College of Aerospace and Civil Engineering, Harbin Engineering University, 150001 Harbin, China

ARTICLE INFO

Article history:
Received 4 February 2021
Received in revised form 12 March 2021
Accepted 26 April 2021
Available online 30 April 2021

Keywords:
Acoustic metamaterials
Low-frequency sound barriers
High-performance ventilation
Acoustic transparency

ABSTRACT

Metamaterials enabling multifunctional wave control have long attracted great interest, but remain largely unexplored in ventilation-required settings. Using the space-coiling strategy, we design and fabricate a compact acoustic meta-structure consisting of labyrinth resonators arranged around a central air passage. Such meta-structures provide a promising route to design well-ventilated and simultaneously highly-effective sound-proofing barriers allowing broadband (about one octave band) transmission loss up to almost 30 dB in the range of 660–1200 Hz. More interestingly, due to the interferences between the forward propagating waves and those re-radiated by the surrounding resonators, some asymmetric Fano-like resonances are observed appearing in the transmission gap. This Fano-like resonance is very useful to open a high transmission window at frequencies of interest by changing the length of coiled-up channels. Our findings are both numerically and experimentally verified, which may stimulate multifunctional applications, such as broadband sound insulation with high transmission loss and tunable acoustic communication, especially in ventilation-required environments.

1. Introduction

Noise control has attracted long-lasting interest owing to its extensive applications in industrial and living fields [1]. Limited by the mass law, this task is rather challenging at low frequencies if one resorts to conventional acoustic barriers that have to be extremely bulky and thus unpractical in engineering. Fortunately, the advent of metamaterials and metasurfaces [2,3], leads a highly effective way enabling a reduction of barriers thickness down to reachable and even deep-subwavelength scales [4–8]. The past decades have witnessed lots of worthwhile endeavors targeted for sound-proofing metamaterials and structures, such as micro-perforated panel absorbers [9,10], mass-decorated membranes/plates [11–13], foam-filled sandwich panels [14,15] and metasurface-based absorbers [16–21], just to name a few. In spite of the great achievements, however, these schemes all suffer from the drawback of airflow blocking that people have to face, either for daily or special applications requiring, for instance, nature ventilation, heat convection and wind-resistant functionalities, etc.

Blocking low-frequency noise without airflow obstruction, intuitively, these two competing goals are hard to reach a satisfactory trade-off. Because of this, early efforts were limited to only a few industries such as architecture where monotonous facade systems like double-leaf facades and louvers were designed for housing ventilation [22,23]. Some recent efforts in the field of metamaterials, however, constitute a new glance of the possibility for unconventional wave control in ventilated environments. García-Chocano et al. [24], targeted for traffic noise shielding, constructed a sound barrier consisting of microperforated cylindrical shells in meter scales and reported its broadband absorption performance. With tactfully engineered Mie resonances, Cheng et al. [25] have developed an ultra-sparse metasurface that is merely subwavelength-thick but highly reflective for low-frequency sound. Afterwards, based on either reflection or absorption mechanisms, a rapidly growing interest has been attracted to this topic reporting various ventilated acoustic systems, typically including metasurfaces composed of Helmholtz resonators [26–28] and labyrinth-type structures [29–32]. Particularly, Ghaffarivardavagh et al. [30] recently reported

* Corresponding author.
** Corresponding author at: Center for Composite Materials, Harbin Institute of Technology, 150001 Harbin, China.
E-mail addresses: x.he@hrbeu.edu.cn (X. He), wlz@hit.edu.cn (L. Wu).
1 These authors contributed equally.

https://doi.org/10.1016/j.eml.2021.101348
2352-4316/

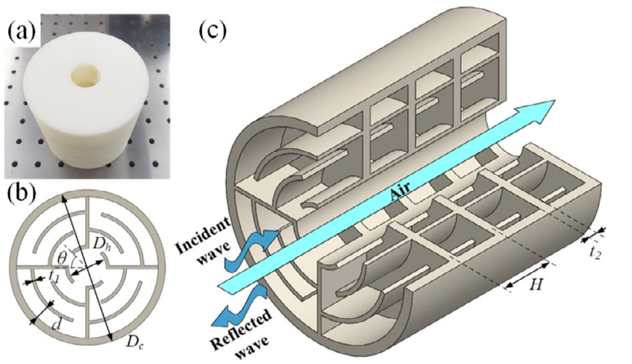

Fig. 1. The engineered sound barriers with ventilation functionality. (a) Photograph of the fabricated sample. Schemes from the (b) front and (c) section views to show the embedded labyrinth cavities. The sample has parameters: lattice period $H = 24$ mm, cylinder diameter $D_c = 100$ mm, hole diameter $D_h = 24$ mm, opening angle of cavity inlet $\theta = \pi/4$, separation between neighbor partitions $d = 9$ mm, and partition thickness $t_1 = 2$ mm and $t_2 = 4$ mm.

a spiral coiling metamaterial that comprises nearly 60% open area for air flow. This structure was demonstrated useful for reducing harmonic industrial noise by employing the narrow band Fano-like interference spectrum.

One ever-lasting goal in noise control engineering is to reduce structural complexity, to lower and widen the sound shielding bands, and even to expand multifunctional applications [30,32,33]. Though progresses have been reported, most recent efforts are still bound to a single function, suffering from either narrow bandwidth, low transmission loss or very limited functionality. In view of this, inspired by the space-coiling strategy, this work reports a carefully engineered sound barrier that not only has compact structure but also enables broadband sound insulation at low frequencies. Furthermore, we investigate the acoustically induced transparency (AIT) phenomena of hybrid model that contains two detuned labyrinth resonators in the unit cell. Through changing the length of coiled channels, it is possible to tune a narrow transmission window to any desired frequencies in the forbidden band, which may facilitate multifunctional applications beyond sound-proofing realm, such as tunable sound transmission and communications.

2. Results and discussion

2.1. Design of ventilated sound barriers

Fig. 1(a) shows a photography of our sample fabricated with the 3D printing technique, from which a circular passage allowing air flowing is clearly seen. For a better illustration of the internal structures, we additionally provide the front and section views in Fig. 1(b) and (c) showing some folded air cavities separated by polymer partitions. The front view shows that each layer is divided into four labyrinth cavities that are coupled together through the central air passage (of diameter D_h). Meanwhile, along the axis several unit cells (of lattice period H) pile up to form an acoustic metamaterial capable of both nature ventilation and sound insulation. As illustrated in Fig. 1(c), when sound waves enter into the engineered meta-structure, their interaction with the re-radiated waves by the surrounding resonators, if destructive-interfered, will impede waves to propagate.

2.2. Broadband sound-proofing performance

To demonstrate the sound isolation performance we calculate, using the COMSOL Multiphysics software, the band diagram and transmission spectrum of the quasi-one-dimensional problem. For the air, the involved parameters are the mass density $\rho_0 = 1.29$ kg/m^3 and speed of sound $c_0 = 343$ m/s. Besides, it is reasonable to assume the polymer partitions as sound rigid walls since their impedance is far larger than that of air. The computed band diagram is shown in Fig. 2(a) where the shaded background represents the predicted low-frequency bandgap ranging from 660 Hz to 1200 Hz, almost covering one octave band. Interestingly, near the lower edge of the bandgap appear three flat bands which are attributed to the fundamental resonance of the labyrinth cavities as depicted in the inset of Fig. 2(a). In order to verify these predictions, we next simulate for finite systems containing n layers to compute the sound transmission loss (STL)

$$\mathrm{STL} = 10 \log_{10} (1/\tau) \tag{1}$$

where τ denotes the power transmission coefficient. As rendered in Fig. 2(a), within the bandgap waves are rapidly attenuated with the increasing of layers. The STL is averagely above 30 dB with only four layers ($n = 4$), which will be selected in this study in consideration of a balance between the sample thickness and sound isolation performance. For a single layer ($n = 1$), what clearly stands out is the appearance of Fano-like resonance [34,35] which spectrally coincides with the flat bands. The increasing layers complicate this Fano-like profile but preserve the typical asymmetric features, i.e., showing both enhanced transmission and enhanced reflection within a narrow frequency range.

Apart from the STL, our metamaterial barriers can be characterized in terms of effective material properties in that the unit cell is in deep-subwavelength scales. Inspired by the work of Fokin et al. [36], we employ the retrieval method to extract effective properties of acoustic metamaterials which, put simply, equates two systems if they show identical transmission and reflection characteristics. Finite element simulations enable us to solve transmission problems characterized by reflection coefficient R and transmitted coefficient T. With these two transmission parameters, we can derive the effective acoustic impedance and refractive index, and finally extract the effective properties, i.e., mass density ρ_{eff} and bulk modulus K_{eff}, via the standard method.

Now, this retrieval method is employed to investigate the influence of some structural parameters, typically including the lattice period H and hole diameter D_h. Except these two variables, all other parameters used in the simulations remain the same as studied in Fig. 2(a). As shown in Fig. 2(b)–(e), in both scenarios we can observe some frequency ranges within which the effective bulk modulus K_{eff} becomes negative, while the extracted density ρ_{eff}, though showing Fano-like resonance, still keeps being positive. Sound cannot propagate within this single-negative band, but instead the imaginary wavenumber forces it to be evanescent waves. Note that $H = 24$ mm [see Fig. 2(b)] is exactly the case we studied in Fig. 2(a). Indeed, a comparison between Fig. 2(a) and (b) reveals that this single-negative feature is well captured by the bandgap, indicating that such negative response actually originates from monopolar resonance as reported in Ref. [37]. In terms of parametric influence, a closer look to Fig. 2(b)–(e) shows that the lattice period has neglectable influence on the bandgap, while the size of ventilation holes slightly matters, which is understandable in that the parameters merely slightly change the length of folded channel, and consequently resulting a mild cavity resonance shifting (see Supplemental Material, Fig. S1). The decrease of hole diameter tends to increase the transmission loss, but on the other hand will deteriorate the ventilation performance. A trade-off has to be made between the two competing goals. This goal can be otherwise achieved by properly increasing the number of unit cell layers (see Supplemental Material, Fig. S2).

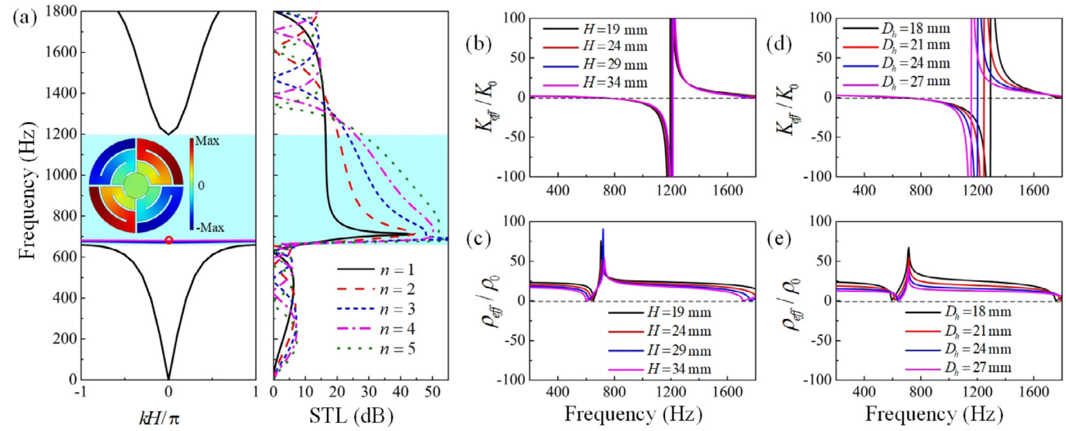

Fig. 2. Sound insulation performance of the ventilated barriers. (a) Calculated band diagram and STL spectra for barriers containing n layers. The shaded background presents the bandgap. One typical eigenfield is depicted in the inset at the selected red point. Parameter dependence of the effective bulk modulus K_{eff} and effective density ρ_{eff} for two scenarios: variation of lattice period H [(b) and (c)] and hole diameter D_h [(d) and (e)]. The results are normalized to the material parameters of air, i.e., the bulk modulus K_0 and mass density ρ_0. The zero-value dashed lines serve as a guide to see the negative response. (For interpretation of the references to color in this figure legend, the reader is referred to the web version of this article.)

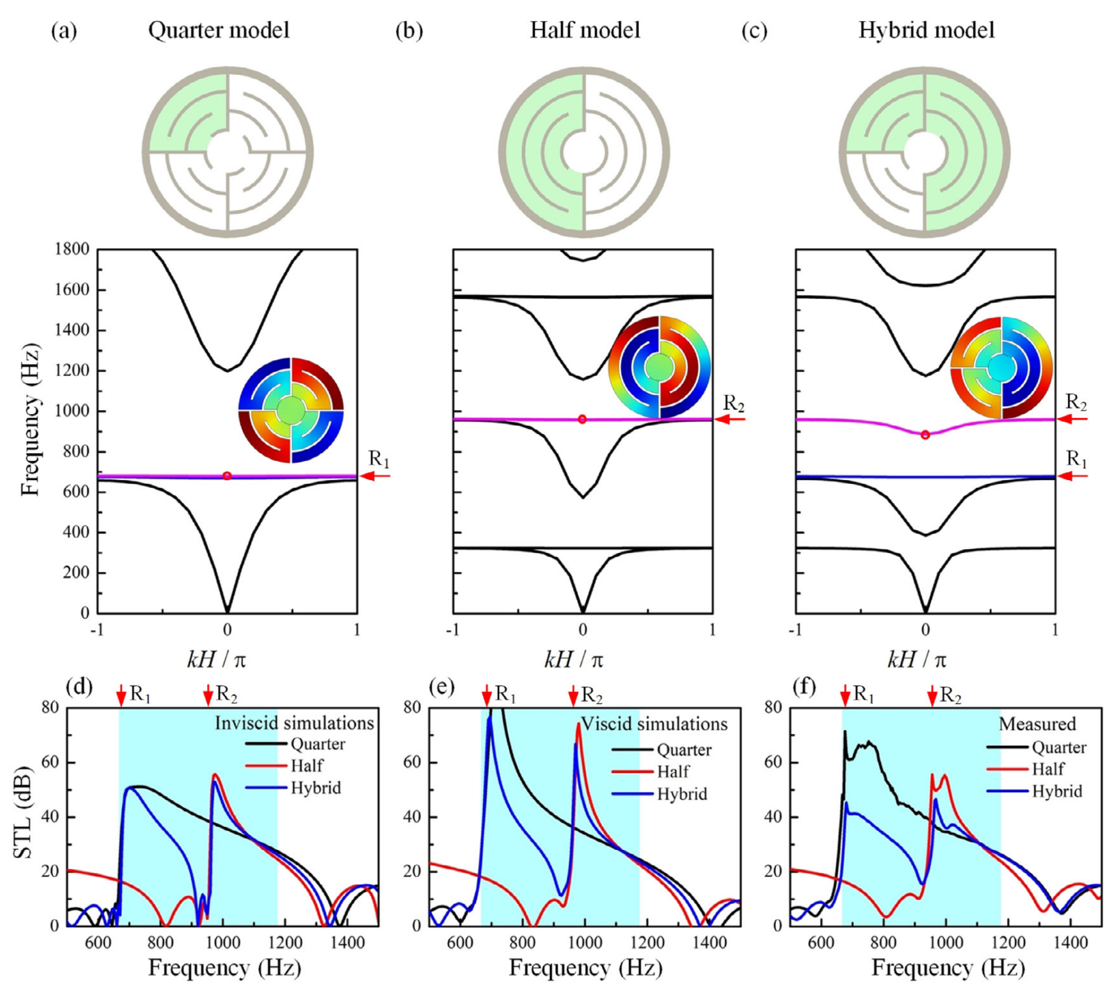

Fig. 3. Enhanced transmission associated with the Fano resonance induced acoustic transparency. (a)–(c) Schematic and band diagrams for various metamaterials containing different labyrinth cavities, i.e., quarter, half and hybrid models. The insets show typical eigenfields for the selected points on the flat bands. All share the same color bar as in Fig. 2(a). (d)–(f) Numerically calculated and experimentally measured STL curves for the three metamaterials. Both inviscid (d) and viscid (e) simulations are implemented to clarify the visco-thermal influence. The shaded background hints the bandgap of the hybrid model. (For interpretation of the references to color in this figure legend, the reader is referred to the web version of this article.)

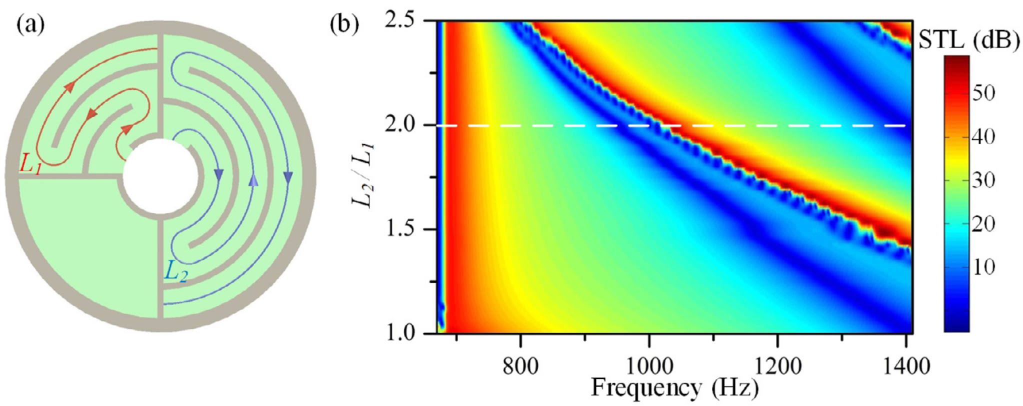

Fig. 4. (a) Schematic diagram of a hybrid model consisting of a quarter cavity (channel length L_1) and a variable cavity of length L_2. (b) Inviscid STL spectra of hybrid models showing the dependence of acoustic transparent window on channel's length ratio L_2/L_1. The dashed line indicates a hybrid model similar to the one studied in Fig. 3(c) containing two types of labyrinth cavities, i.e., the quarter and half ones.

2.3. Fano resonance induced acoustic transparency

Through tuning the labyrinth cavities, the proposed metamaterials are capable of achieving more interesting functionality such as the Fano resonance induced transparency. As illustrated in Fig. 3, beyond the barrier studied before, two additional structures are further explored which differ from each other in their partition patterns as highlighted in green. For clarity, these three structures from left to right are named as quarter model, half model and hybrid model, respectively. We begin by computing the band diagrams to unravel their resonance properties [see Fig. 3(a)–(c)]. Note, when compared with the quarter model, the half model produces more bands within the frequency range studied. Due to the channel length doubling, we see the fundamental resonance is red-shifted from 679 Hz [first flat band in Fig. 3(a)] to 322 Hz [first flat band in Fig. 3(b)], meanwhile in Fig. 3(b) a second flat band corresponding to one-order higher resonance appears at 958 Hz, falling into the frequency range of interest. For the hybrid model containing both labyrinth cavities, Fig. 3(c) shows a somewhat hybrid band structure that possesses some main features as in Fig. 3(a) and (b), but is not merely a simple superposition of the quarter and half models. Above the first flat band we observe a broad bandgap that is spectrally almost the same as that of quarter model. Inside this bandgap the right half labyrinth cavity additionally produces a resonance-induced flat band [see the inset in Fig. 3(c)] locating at about the mid-gap point. As discussed in Fig. 2, such kind of flat band is closely associated with the asymmetric Fano profile in the STL spectra, which is likely to open a sound transmission window inside the bandgap.

To verify this, for the three models we calculate their STL curves in the absence of visco-thermal damping, as rendered in Fig. 3(d). It is clear seen that, in all scenarios, some Fano-like response was excited at frequencies (see labels R_1 and R_2) that match well with the flat band predictions. Remarkably, thanks to the enhanced transmission associated with Fano resonance, there appears an acoustic transparent window inside the bandgap at about 920 Hz. In practice, visco-thermal loss is unavoidable for structures consisting of narrow channels. We therefore implement a group of viscid simulations as shown in Fig. 3(e). In comparison with the inviscid results, visco-thermal damping tends to enhance the transmission loss especially when resonance happens, nevertheless it cannot significantly affect the main spectral features predicted by the inviscid simulations, such as the wide forbidden band and the mid-gap transmission window. In a step further, experiments were performed to validate our numerical predictions. All the three samples were fabricated via 3D printing technique, and were properly installed and measured according to ASTM standard [38]. As displayed in Fig. 3(f), due to the machining errors, the resonance response is slightly different in comparison with simulations, but overall a good agreement is observed between the calculated and measured spectra. To be specific, for the quarter model, the measured results consolidate the predicted low-frequency bandgap whose transmission loss averagely reaches 30 dB in one octave band. Once hybridized with different labyrinth cavities, within this bandgap, an acoustic transmission window is opened at around 920 Hz, matching well with our band structure and STL predictions.

We now demonstrate that our metamaterials enjoy an advantage of facile tunability, i.e., acoustic transmission window can be spectrally shifted by changing the length of folded channels. Again, this exploration is based on a hybrid model whose quarter cavity (of channel length L_1) remains unchanged, but the other labyrinth cavity has a variable channel length L_2, which is achievable by moving the partition to desired positions, see the sketch in Fig. 4(a). Fig. 4(b) maps the STL spectra of this hybrid model in dependence of its channel's length ratio L_2/L_1. Note that the white dashed line corresponds to a scenario similar to the hybrid model studied in Fig. 3(c) whose transparent window locates at 920 Hz. Beyond this, with the decreasing of channel's length ratio, the Fano-like resonance experiences a blue-shifting within a wide frequency range. This together with the broadband sound isolation performance may stimulate multifunctional applications in ventilation environments.

3. Conclusions

In summary, we have designed and fabricated a subwavelength metamaterial barrier that enables multifunctional sound control. This sound barrier is carefully designed using the space-coiling strategy whose labyrinth resonators are circularly arranged to form a passage allowing airflow to pass through it. Both the calculated transmission loss and the extracted effective properties predict its low-frequency sound insulation performance, covering almost one octave band from 660 Hz to 1200 Hz. Beyond blocking sound waves, such labyrinth-type metamaterial is demonstrated having Fano-like resonance features which, if cleverly harnessed, is very useful to open acoustic transmission window in the bandgap. By changing the folded channel length, it is further shown that this enhanced transmission phenomena can be easily tuned within a wide frequency range. The numerical predictions have been experimentally verified showing good agreement with the measured data. We foresee that our work may inspire multifunctional acoustic applications such as broadband sound insulation and selective wave transmission that are unreachable before on circumstances requiring nature ventilation.

Declaration of competing interest

The authors declare that they have no known competing financial interests or personal relationships that could have appeared to influence the work reported in this paper.

Data availability statement

All the data that support the findings of this study are available from the corresponding author upon reasonable request.

Acknowledgments

This work was supported by the National Natural Science Foundation of China (No. 11702069) and the Postdoctoral Science Foundation of China (No. 2019M660070).

Appendix A. Supplementary data

Supplementary material related to this article can be found online at https://doi.org/10.1016/j.eml.2021.101348.

References

[1] David A. Bies, Colin Hansen, Carl Howard, Engineering Noise Control, CRC press, 2017.
[2] Zhengyou Liu, Xixiang Zhang, Yiwei Mao, Y.Y. Zhu, Zhiyu Yang, C.T. Chan, Ping Sheng, Locally resonant sonic materials, Science 289 (2000) 1734–1736, http://dx.doi.org/10.1126/science.289.5485.1734.
[3] Nanfang Yu, Patrice Genevet, Mikhail A. Kats, Francesco Aieta, Jean-Philippe Tetienne, Federico Capasso, Zeno Gaburro, Light propagation with phase discontinuities: Generalized laws of reflection and refraction, Science 334 (2011) 333–337, http://dx.doi.org/10.1126/science.1210713.
[4] Min Yang, Ping Sheng, Sound absorption structures: From porous media to acoustic metamaterials, Annu. Rev. Mater. Res. 47 (2017) 83–114, http://dx.doi.org/10.1146/annurev-matsci-070616-124032.
[5] Yan-Feng Wang, Yi-Ze Wang, Bin Wu, Weiqiu Chen, Yue-Sheng Wang, Tunable and active phononic crystals and metamaterials, Appl. Mech. Rev. 72 (2020) 040801, http://dx.doi.org/10.1115/1.4046222.
[6] Yong Li, Badreddine M. Assouar, Acoustic metasurface-based perfect absorber with deep subwavelength thickness, Appl. Phys. Lett. 108 (2016) 063502, http://dx.doi.org/10.1063/1.4941338.
[7] Penglin Gao, Alfonso Climente, José Sánchez-Dehesa, Linzhi Wu, Theoretical study of platonic crystals with periodically structured N-beam resonators, J. Appl. Phys. 123 (2018) 091707, http://dx.doi.org/10.1063/1.5009170.
[8] Penglin Gao, Alfonso Climente, José Sánchez-Dehesa, Linzhi Wu, Single-phase metamaterial plates for broadband vibration suppression at low frequencies, J. Sound Vib. 444 (2019) 108–126, http://dx.doi.org/10.1016/j.jsv.2018.12.022.
[9] Soon-Hong Park, Acoustic properties of micro-perforated panel absorbers backed by Helmholtz resonators for the improvement of low-frequency sound absorption, J. Sound Vib. 332 (2013) 4895–4911, http://dx.doi.org/10.1016/j.jsv.2013.04.029.
[10] Fe Wu, Yong Xiao, Dianlong. Yu, Honggang Zhao, Yang Wang, Jihong Wen, Low-frequency sound absorption of hybrid absorber based on micro-perforated panel and coiled-up channels, Appl. Phys. Lett. 114 (2019) 151901, http://dx.doi.org/10.1063/1.5090355.
[11] Z. Yang, Jun Mei, Min Yang, N.H. Chan, Ping Sheng, Membrane-type acoustic metamaterial with negative dynamic mass, Phys. Rev. Lett. 101 (2008) 204301, http://dx.doi.org/10.1103/PhysRevLett.101.204301.
[12] Ni Sui, Xiang Yan, Tai-Yun Huang, Jun Xu, Fuh-Gwo Yuan, Yun Jing, A lightweight yet sound-proof honeycomb acoustic metamaterial, Appl. Phys. Lett. 106 (2015) 171905, http://dx.doi.org/10.1063/1.4919235.
[13] Tai-Yun Huang, Chen Shen, Yun Jing, Membrane- and plate-type acoustic metamaterials, J. Acoust. Soc. Am. 139 (2016) 3240–3250, http://dx.doi.org/10.1121/1.4950751.
[14] Dong-Wei Wang, Li Ma, Sound transmission through composite sandwich plate with pyramidal truss cores, Compos. Struct. 164 (2017) 104–117, http://dx.doi.org/10.1016/j.compstruct.2016.11.088.
[15] M.P. Arunkumar, Jeyaraj Pitchaimani, K.V. Gangadharan, M.C. Leninbabu, Vibro-acoustic response and sound transmission loss characteristics of truss core sandwich panel filled with foam, Aerosp. Sci. Technol. 78 (2018) 1–11, http://dx.doi.org/10.1016/j.ast.2018.03.029.
[16] Junfei Li, Wenqi Wang, Yangbo Xie, Bogdan-Ioan Popa, Steven A. Cummer, A sound absorbing metasurface with coupled resonators, Appl. Phys. Lett. 109 (2016) 091908, http://dx.doi.org/10.1063/1.4961671.
[17] Houyou Long, Chen Shao, Chen Liu, Ying Cheng, Xiaojun Liu, Broadband near-perfect absorption of low-frequency sound by subwavelength metasurface, Appl. Phys. Lett. 115 (2019) 103503, http://dx.doi.org/10.1063/1.5109826.
[18] Yi Fang, Xin Zhang, Jie Zhou, Acoustic porous metasurface for excellent sound absorption based on wave manipulation, J. Sound Vib. 434 (2018) 273–283, http://dx.doi.org/10.1016/j.jsv.2018.08.003.
[19] Sibo Huang, Zhiling Zhou, Dongting Li, Tuo Liu, Xu Wang, Jie Zhu, Yong Li, Compact broadband acoustic sink with coherently coupled weak resonances, Sci. Bull. 65 (2020) 373–379, http://dx.doi.org/10.1016/j.scib.2019.11.008.
[20] Changru Chen, Zhibo Du, Gengkai Hu, Jun Yang, A low-frequency sound absorbing material with subwavelength thickness, Appl. Phys. Lett. 110 (2017) 221903, http://dx.doi.org/10.1063/1.4984095.
[21] Antonio A. Fernández-Marín, Noé Jiménez, Jean-Philippe Groby, José Sánchez-Dehesa, Vicente Romero-García, Aerogel-based metasurfaces for perfect acoustic energy absorption, Appl. Phys. Lett. 115 (2019) 061901, http://dx.doi.org/10.1063/1.5109084.
[22] Egzon Bajraktari, Josef Lechleitner, Ardeshir Mahdavi, The sound insulation of double facades with openings for natural ventilation, Build. Acoust. 22 (2015) 163–176, http://dx.doi.org/10.1260/1351-010X.22.3-4.163.
[23] Nicolò Zuccherini Martello, Patrizio Fausti, Andrea Santoni, Simone Secchi, The use of sound absorbing shading systems for the attenuation of noise on building façades. An experimental investigation, Buildings 5 (2015) 1346–1360, http://dx.doi.org/10.3390/buildings5041346.
[24] Victor M. García-Chocano, Suitberto Cabrera, José Sánchez-Dehesa, Broadband sound absorption by lattices of microperforated cylindrical shells, Appl. Phys. Lett. 101 (2012) 184101, http://dx.doi.org/10.1063/1.4764560.
[25] Y. Cheng, C. Zhou, B.G. Yuan, D.J. Wu, Q. Wei, X.J. Liu, Ultra-sparse metasurface for high reflection of low-frequency sound based on artificial Mie resonances, Nature Mater. 14 (2015) 1013–1019, http://dx.doi.org/10.1038/nmat4393.
[26] Xiang Yu, Zhenbo Lu, Li Cheng, Fangsen Cui, On the sound insulation of acoustic metasurface using a sub-structuring approach, J. Sound Vib. 401 (2017) 190–203, http://dx.doi.org/10.1016/j.jsv.2017.04.042.
[27] Jae Woong Jung, Jae Eun Kim, Jin Woo Lee, Acoustic metamaterial panel for both fluid passage and broadband soundproofing in the audible frequency range, Appl. Phys. Lett. 112 (2018) 041903, http://dx.doi.org/10.1063/1.5004605.
[28] Sanjay Kumar, Tiong Bang Xiang, Heow Pueh Lee, Ventilated acoustic metamaterial window panels for simultaneous noise shielding and air circulation, Appl. Acoust. 159 (2020) 107088, http://dx.doi.org/10.1016/j.apacoust.2019.107088.
[29] Jieun Yang, Joong Seok Lee, Hyeong Rae Lee, Yeon June Kang, Yoon Young Kim, Slow-wave metamaterial open panels for efficient reduction of low-frequency sound transmission, Appl. Phys. Lett. 112 (2018) 091901, http://dx.doi.org/10.1063/1.5003455.
[30] Reza Ghaffarivardavagh, Jacob Nikolajczyk, Stephan Anderson, Xin Zhang, Ultra-open acoustic metamaterial silencer based on Fano-like interference, Phys. Rev. B 99 (2019) 024302, http://dx.doi.org/10.1103/PhysRevB.99.024302.
[31] Hai-long Zhang, Yi-fan Zhu, Bin Liang, Jing Yang, Jun Yang, Jian-chun Cheng, Omnidirectional ventilated acoustic barrier, Appl. Phys. Lett. 111 (2017) 203502, http://dx.doi.org/10.1063/1.4993891.
[32] Man Sun, Xinsheng Fang, Dongxing Mao, Xu Wang, Yong Li, Broadband acoustic ventilation barriers, Phys. Rev. Applied 13 (2020) 044028, http://dx.doi.org/10.1103/PhysRevApplied.13.044028.
[33] Sanjay Kumar, Heow Pueh Lee, Recent advances in acoustic metamaterials for simultaneous sound attenuation and air ventilation performances, Crystals 10 (2020) 686, http://dx.doi.org/10.3390/cryst10080686.
[34] Mikhail F. Limonov, Mikhail V. Rybin, Alexander N. Poddubny, Yuri S. Kivshar, Fano resonances in photonics, Nat. Photon. 11 (2017) 543–554, http://dx.doi.org/10.1038/nphoton.2017.142.
[35] M. Amin, A. Elayouch, M. Farhat, M. Addouche, A. Khelif, H. Bağcı, Acoustically induced transparency using Fano resonant periodic arrays, J. Appl. Phys. 118 (2015) 164901, http://dx.doi.org/10.1063/1.4934247.
[36] Vladimir Fokin, Muralidhar Ambati, Cheng Sun, Xiang Zhang, Method for retrieving effective properties of locally resonant acoustic metamaterials, Phys. Rev. B 76 (2007) 144302, http://dx.doi.org/10.1103/PhysRevB.76.144302.
[37] Jensen Li, C.T. Chan, Double-negative acoustic metamaterial, Phys. Rev. E 70 (2004) 055602, http://dx.doi.org/10.1103/PhysRevE.70.055602.
[38] ASTM E2611-19, Standard Test Method for Normal Incidence Determination of Porous Material Acoustical Properties Based on the Transfer Matrix Method, ASTM, 2019.